High Resolution Characterization of Formamidopyrimidine-DNA Glycosylase Interaction with Its Substrate by Chemical Cross-linking and Mass Spectrometry Using Substrate Analogs*

Maria Rogacheva[‡], Alexander Ishchenko[§], Murat Saparbaev[§], Svetlana Kuznetsova[‡], and Vasily Ogryzko[¶][1]

From the [‡]Laboratory of Nucleic Acids Chemistry, Department of Chemistry, Moscow State University, Moscow 119992, Russia and the [§]DNA Repair and [¶]Molecular Epigenetics Groups, CNRS UMR 8126, University Paris-Sud, Institut Gustave Roussy, 94805 Villejuif Cedex, France

Escherichia coli formamidopyrimidine-DNA glycosylase (Fpg) and human 8-oxoguanine-DNA glycosylase (hOgg1) initiate the base excision repair pathway for 7,8-dihydro-8-oxoguanine (8-oxoG) residues present in DNA. Recent structural and biochemical studies of Fpg-DNA and hOgg1-DNA complexes point to the existence of extensive interactions between phosphate groups and amino acids. However, the role of these contacts and their physiological relevance remains unclear. In the present study, we combined chemical cross-linking and electrospray ionization mass spectrometry (ESI/MS/MS) approaches to identify interacting residues in the Fpg-DNA and hOgg1-DNA complexes. The active centers of Fpg and hOgg1 were cross-linked with a series of reactive oligonucleotide duplexes containing both a single 8-oxoG residue and an *O-ethyl*-substituted pyrophosphate internucleotide (SPI) group at different positions in duplex DNA. The cross-linking efficiency reached 50% for Fpg and 30% for hOgg1. We have identified seven phosphate groups on both strands of the DNA duplex specifically interacting with nucleophilic amino acids in Fpg, and eight in hOgg1. MS/MS analysis of the purified proteolytic fragments suggests that lysine 56 of Fpg and lysine 249 of hOgg1 cross-link to the phosphate located 3′ to the 8-oxoG residue. Site-specific mutagenesis analysis of Fpg binding to DNA substrate confirms the conclusions of our approach. Our results are consistent with crystallographic data on the Fpg-DNA complex and provide new data on the hOgg1-DNA interaction. The approach developed in this work provides a useful tool to study pro- and eukaryotic homologues of Fpg as well as other repair enzymes.

Escherichia coli formamidopyrimidine-DNA glycosylase (Fpg)[2] (also known as MutM) and human 8-oxoguanine-DNA glycosylase (hOgg1) are DNA repair enzymes that catalyze the removal of 7,8-dihydro-8-oxoguanine (8-oxoG) residues from DNA (1–3). 8-OxoG is the major mutagenic base damage generated in DNA by reactive oxygen species produced in aerobic respiration and after cell injury or exposure to physical and chemical oxygen radical-forming agents (4). 8-OxoG is a miscoding lesion, because it pairs preferentially with adenine instead of cytosine and induces G·C → T·A transversions *in vivo* and *in vitro* (5, 6). Thus the Fpg and hOgg1 DNA glycosylases are important in prevention of the mutagenic effects of 8-oxoG residues present in DNA and maintenance of genome integrity.

To date, most studies have focused on the interactions of Fpg and hOgg1 with oxidized bases, and little attention has been paid to contacts with phosphate groups in damaged DNA. However, it is evident that interactions of the DNA glycosylases with DNA phosphate groups are critical for the target search along DNA and base lesion recognition. It has been shown that the interaction of Fpg and hOgg1 with damaged DNA causes significant conformational changes in helix structure, such as partial denaturation, widening of the minor groove, sharp kinking of the DNA backbone at the lesion site, and flipping-out of the oxidized base from the DNA duplex (7, 8). Such enzyme-induced changes in DNA duplex structure occur mostly through specific contacts between amino acids in the active centers of Fpg and hOgg1, on the one hand, and DNA phosphate groups in the specific protein-DNA complexes, on the other (9, 10). In contrast to the nonspecific weak interactions of Fpg and hOgg1 with phosphates found in non-damaged DNA, complex formation between DNA glycosylase and damaged DNA takes on a cooperative character and involves separate directly interacting groups (9, 10). However, detailed study of such interactions has not yet been carried out.

In this work, we examined specific contacts between DNA phosphate groups and nucleophilic amino acids of Fpg and hOgg1 in the specific enzyme-substrate complexes, under physiological conditions, using combined cross-linking and proteomic approaches. Chemical cross-linking is widely used to study protein-DNA interactions. The method provides information about the geometry of the contacts and the binding centers of the interacting molecules, and also allows identifica-

[1] To whom correspondence should be addressed. Tel.: 33-14211-6525; Fax: 33-14211-6525; E-mail: ogryzko@igr.fr.

[2] The abbreviations used are: Fpg, formamidopyrimidine-DNA glycosylase; MS, mass spectrometry; ESI, electrospray ionization; *N*-MeIm, *N*-methylimidazole; SPI, reactive *O-ethyl*-substituted pyrophosphate internucleotide group; 8-oxoG, 7,8-dihydro-8-oxoguanine; hOgg1, human 8-oxoguanine-DNA glycosylase 1; HPLC, high pressure liquid chromatography; MES, 4-morpholineethanesulfonic acid.

tion of single atoms or groups of atoms involved in the specific interaction in aqueous solutions (11). Electrospray ionization mass spectrometry (ESI-MS) is a technique that has been used in cross-linking studies for peptide identification and sequencing (12). The principal advantage of ESI-MS is an ability to accurately determine the masses of molecules analyzed in a complex mixture. The ability of most modern mass spectrometers to fragment parent ions (MS/MS) provides highly reliable information on their identity. In this work, we present two alternative strategies combining cross-linking and ESI/MS/MS to identify the amino acids of 8-oxoguanine-DNA glycosylases interacting with DNA phosphate groups under physiological conditions. The role of phosphate-protein contacts in substrate recognition is also discussed.

EXPERIMENTAL PROCEDURES

Oligonucleotides—Oligonucleotide DNA duplexes I–XI used in this study are shown in Fig. 1. The 8-oxoG residue was introduced into the oligonucleotides by a standard phosphoramidite procedure using an Applied Biosystems 380B DNA synthesizer and commercially available 3′-phosphoramidite of modified 2′-deoxyguanosine (Glenn Research, Sterling, VA). Modified oligonucleotides containing internucleotide SPI groups at the positions indicated by *arrows* in Fig. 1*A* were made by template-directed chemical ligation as described (13). Briefly, equimolar amounts of the *O-ethyl*-substituted 3′-phosphate upstream oligonucleotide, the 5′-[^{32}P]phosphate downstream oligonucleotide to be ligated, and a complementary 22-mer oligonucleotide used as a template to appose the two phosphate groups (the total oligonucleotide concentration was 10^{-3} M), dissolved in 20 μl of buffer A containing 0.05 M MES-HCl (pH 6.0), 0.02 M MgCl$_2$, were heated to 80 °C for 2 min and slowly cooled. The mixture thus obtained was treated with 0.2 M water-soluble carbodiimide for 72 h at 10 °C in the dark. Ligation products carrying a pOC_2H_5-[^{32}P]phosphate-substituted pyrophosphate group at the ligation site (Fig. 1*A*) were isolated by electrophoresis on a 20% polyacrylamide gel containing 7 M urea, followed by elution with 2 M LiClO$_4$ and precipitation with 5 volumes of acetone. Ligation efficiency was dependent on the nature of nucleotides at the ligation site and varied between 12 and 60%. The influence of the nature of nucleotides at the ligation site on the ligation efficiency was noted earlier (13, 14).

The SPI-containing oligonucleotide of DNA duplex IV used for mass spectrometry experiments was synthesized on a preparative scale. 20 nmol of the oligonucleotide with 5′-phosphate, 20 nmol of the oligonucleotide with 3′-ethylphosphate, and 22 nmol of the DNA template oligonucleotide in 50 μl of buffer A were annealed as described above. Carbodiimide (5 mg) was added and the solution was thoroughly vortexed and incubated at 10 °C for 72 h. SPI-containing oligonucleotide was isolated by electrophoresis on a 20% polyacrylamide gel containing 7 M urea. The gel was examined by UV shadowing, the bands corresponding to the ligation product were excised, and the oligonucleotide was recovered by passive elution at room temperature as described above.

All oligonucleotides were tested by HPLC and, if necessary, purified by HPLC or denaturing 20% PAGE. Oligonucleotides were 5′-^{32}P-labeled as described (15). DNA duplexes I–XI were

obtained by annealing (heating to 40 °C for 2 min and slow cooling) the respective SPI-containing oligonucleotides with an equimolar amount of the complementary strand. The reactivity of these modified duplexes was confirmed as described earlier (16). DNA duplexes I–XI were selectively cleaved under the action of aqueous solutions of *N*-MeIm or ethylenediamine at pH 8.0 according to the mechanism of nucleophilic substitution at the phosphorus atom as was determined previously (16). DNA duplex XII contained no internal SPI groups.

Protein Preparation—The non-labeled wild-type and mutant Fpg and hOgg1 proteins were purified as previously described (17, 18). In the present work, to facilitate MS data manipulation, the amino acid sequence of the Fpg protein was numbered beginning from P1, E2 ... Lys^{56} etc. Site-directed mutations R53G, R54G, K56R, and K56G within the Fpg coding sequence in pFPG220 were generated by a site-directed mutagenesis kit (QuikChange® XL, Stratagene) as described (19, 20). To obtain stable isotope-labeled DNA glycosylases, the cDNAs of Fpg and hOgg1 were cloned into vectors pET11a and pET28c(+) (Novagen, Madison, WI), respectively, and transformed into the *E. coli* strain Rosetta (DE3) (Invitrogen SARL, Gergy Pontoise, France). M9 medium, containing either ^{14}NH$_4$Cl or ^{15}NH$_4$Cl supplemented with 50 μg/ml of appropriate antibiotics was inoculated with overnight culture and incubated at 18 °C until $A_{600\ nm} = 1.0$. At this point, isopropyl 1-thio-β-D-galactopyranoside was added to a final concentration of 0.5 mM, and the proteins were overproduced for 6 h at 37 °C. Homogeneity of the protein preparations was verified by SDS-PAGE.

Chemical Cross-linking—Sample manipulations for mass spectrometry analyses were performed in methanol-washed tubes to reduce polymer contamination. Chemical cross-linking of Fpg and hOgg1 to modified oligonucleotide duplexes I–X was performed on both analytical and preparative scales. For analytical scale cross-linking, 1–10 nM Fpg and 10–100 nM hOgg1 were incubated with 2–20 fmol of oligonucleotide duplexes in 20 μl of buffer B containing 25 mM Hepes-KOH, pH 7.6, 100 mM KCl, 5 mM 2-mercaptoethanol, 2 mM Na$_2$EDTA, 0.1% (w/v) bovine serum albumin, 6% (v/v) glycerol, and 0.05 M *N*-methylimidazole (*N*-MeIm) for 14 h at 0, 22, or 37 °C unless otherwise stated. In all DNA duplexes only the disubstituted phosphate group of the modified pyrophosphate residue was ^{32}P-labeled (Fig. 1*A*). Reaction mixtures were analyzed by electrophoresis on a 12% SDS-PAGE gel after heating samples in 0.1% SDS, 1 M 2-mercaptoethanol solution at 95 °C. Gels were exposed to a Fuji FLA-3000 PhosphorScreen and analyzed using Image Gauge version 3.12 software. Cross-linking efficiency was determined as the ratio of the amount of DNA-enzyme covalent complex to the total amount of the DNA (conjugate plus unbound DNA).

In the preparative scale experiment, 42.5 μM Fpg or 50 μM hOgg1 were incubated with 20 μM oligonucleotide duplex IV spiked with ^{32}P-labeled DNA in 40 μl of buffer B without bovine serum albumin for 16 h at 37 °C. A small amount of the reaction mixture was separated by 12% SDS-PAGE, and radioactivity was quantified by phosphorimaging. The yields of Fpg-DNA and hOgg1-DNA heteroconjugates were about 50 and 30%, respectively. Cross-linked Fpg and hOgg1 were separated

from free proteins by 12% SDS-PAGE and stained with Sypro-Red and colloidal Coomassie G-250, respectively.

Isolation of Oligonucleotide-hOgg1 Peptide Conjugate—Approximately 20 pmol each of free and cross-linked hOgg1 proteins were cut from the stained preparative gel. The gel slices were minced to cubes of about 1 mm^3 and washed three times with 300 μl of 0.1 M NH$_4$HCO$_3$, 50% acetonitrile at 25 °C for 5 min in 1.5-ml tubes. Gel slices were first dried in 100% acetonitrile for 15 min and then in a SpeedVac for 10 min; they were next allowed to swell in 300 μl of freshly prepared 0.1 M NH$_4$HCO$_3$, 10 mM dithiothreitol at 56 °C for 1 h without shaking. The supernatant was discarded, and the proteins were alkylated in-gel in 300 μl of 55 mM iodoacetamide, 0.1 M NH$_4$HCO$_3$ at room temperature for 45 min in the dark (briefly mixed every 10 min). After alkylation, gel slices were washed and dried as described above.

For trypsin digestion, gel slices were re-hydrated in 25 mM NH$_4$HCO$_3$, 1 mM CaCl$_2$, preincubated on ice for 15 min, and incubated with trypsin (Promega France, Charbonnieres) at a w/w ratio of 1:20 (trypsin:hOgg1) at 37 °C for 16 h. To extract the residual peptides, gel slices were washed in 25 μl of 25 mM NH$_4$HCO$_3$ at 25 °C by shaking at 1400 rpm for 10 min. Supernatant was removed, and gel slices were washed twice with 25 μl of 0.1% formic acid and 50% acetonitrile at 25 °C by shaking at 1400 rpm for 10 min. All the supernatants containing peptides were pooled together and concentrated to 10 μl for mass spectrometry experiments.

Isolation of Oligonucleotide-Fpg Peptide Conjugate—After preparative cross-linking, the reaction mixture was denatured in 0.1% SDS at 95 °C for 2 min, cooled to room temperature, and incubated on ice for 10 min. Proteolytic digestion was performed by the addition of chymotrypsin at a ratio of 1:20 (w/w) for protease:protein. Aliquots of the digestion mixture were analyzed on 12% denaturing PAGE gels (0.5 × TBE, 2 M urea) to ensure complete digestion. Afterward, the sample was loaded onto a 0.5-ml column packed with Q-Sepharose Fast Flow resin (Amersham Biosciences). The column was sequentially washed with 0.2 M NaCl, 0.4 M NaCl, and 1 M NH$_4$HCO$_3$ to remove peptides that were not cross-linked to DNA. The retained material, comprising unreacted oligonucleotides and peptide-oligonucleotide conjugates, was eluted with 2 M NH$_4$HCO$_3$ and then incubated at 95 °C and dried in a SpeedVac concentrator to desalt the sample. Selective cleavage of the phosphoroamide linkage in the heteroconjugate was achieved by treatment with 5% formic acid at room temperature for 30 min.

Mass Spectrometry—The peptide mixtures obtained after protease digestions were analyzed by nano-HPLC (LC Packing) directly coupled to an ion trap mass spectrometer (ThermoFinnigan LCQ Deca XP) equipped with a nanoelectrospray source. The mass spectrometer was run in several different modes. For peptide identification, the ion trap acquired successive sets of 4 scan modes consisting of: full scan MS over the ranges of 200–2000 *m/z*, followed by 3 data-dependent MS/MS scans of the 3 most abundant ions in the full scan. The MS/MS spectra were acquired with a relative collision energy of 35% and exclusion width of 2.0 Da. The spectra were interpreted with the Bioworks software package. Alternatively, for confirmation and quantification of the presence of a particular peptide in the sample, the ion trap was set in a SRM mode. The quantity of the corresponding peptides was estimated by the peak intensity. For the stable isotope experiments, the mass spectrometer was set in a Zoom scan mode to target the area that covers masses of candidate peptides and the isotope-labeled controls. Comparison of experimentally obtained molecular masses of the peptides with theoretically possible peptides formed during trypsin digestion of hOgg1 and chymotrypsin digestion of the Fpg protein was carried out using the program PeptMass.

Electrophoretic Mobility Shift Assay and Determination of the Apparent Dissociation Constants (K_D)—The assay mixture (20 μl final volume) contained ^{32}P-labeled DNA duplex IV at a concentration of 20 pM and Fpg proteins (0.1–12 nM wild-type Fpg or 1–30 nM FpgK56R, or 1–150 nM FpgK56G, Fpg R53G, or FpgR54G) in buffer B without *N*-MeIm. The reactions were performed at 0 °C for 10 min and immediately loaded onto pre-run non-denaturing 10% PAGE gels as described (21, 22). Gel electrophoresis was carried out at 4 °C for 1.5 h. Gels were exposed and analyzed as described above. Binding efficiency was determined as the ratio of the amount of protein-DNA complex to the total amount of DNA (bound and unbound). Assuming that the complexes contained one enzyme molecule per molecule of DNA, the apparent dissociation constant (K_D) can be calculated from the concentrations of free protein ([E]), free DNA (f), and bound protein-DNA complex (1-f) at equilibrium: $K_D = [E] \times f/(1-f)$. If the total concentration of protein [E]$_0$ is close to that of the free protein at equilibrium, $K_D = [E]_0$ when 50% of the DNA is bound by the enzyme (21, 22).

RESULTS

Design and Synthesis of Modified DNA Duplexes—To study specific contacts between DNA phosphate groups and amino acids of the Fpg or hOgg1 proteins, a series of DNA duplexes containing both an 8-oxoG residue and a reactive *O-ethyl*-substituted pyrophosphate internucleotide (SPI) group (Fig. 1*A*) were synthesized by chemical ligation (13). We established previously that nucleic acid fragments containing an SPI group are easily and quantitatively cleaved by primary and secondary amines, including nucleophilic amino acids (16, 23). The reaction mechanism involves nucleophilic attack at the disubstituted phosphorous atom of the SPI group and elimination of an oligonucleotide remnant that contains the 3'-*O*-ethylphosphate derived from the modified phosphate of the pyrophosphate linkage (Fig. 1*B*). The cleavage of the modified group is accompanied by a transfer of the nucleic acid fragment onto the amine or amino acid. As a result, a phosphoamide (P-N) bond is formed. Nucleic acid fragments containing an SPI group may be regarded as phosphorylating reagents, acting on the nucleophil and covalently modifying it with a segment of oligonucleotide from the original DNA or RNA. The selective attack of the nucleophil on the disubstituted phosphorous atom of an SPI group can be explained by the stability of the eliminated group (monoanionphosphate is more stable (p$K_a \sim$ 1), than bianion-phosphate (p$K_a \sim$ 6)) and by a greater steric accessibility of the flipped-out disubstituted phosphate *versus* the trisubstituted phosphate of the SPI group.[3] Phosphoamide covalent bonds are

---

[3] M. V. Rogacheva, A. V. Bochenkova, S. A. Kuznetsova, and A. V. Nemukhin, unpublished observations.
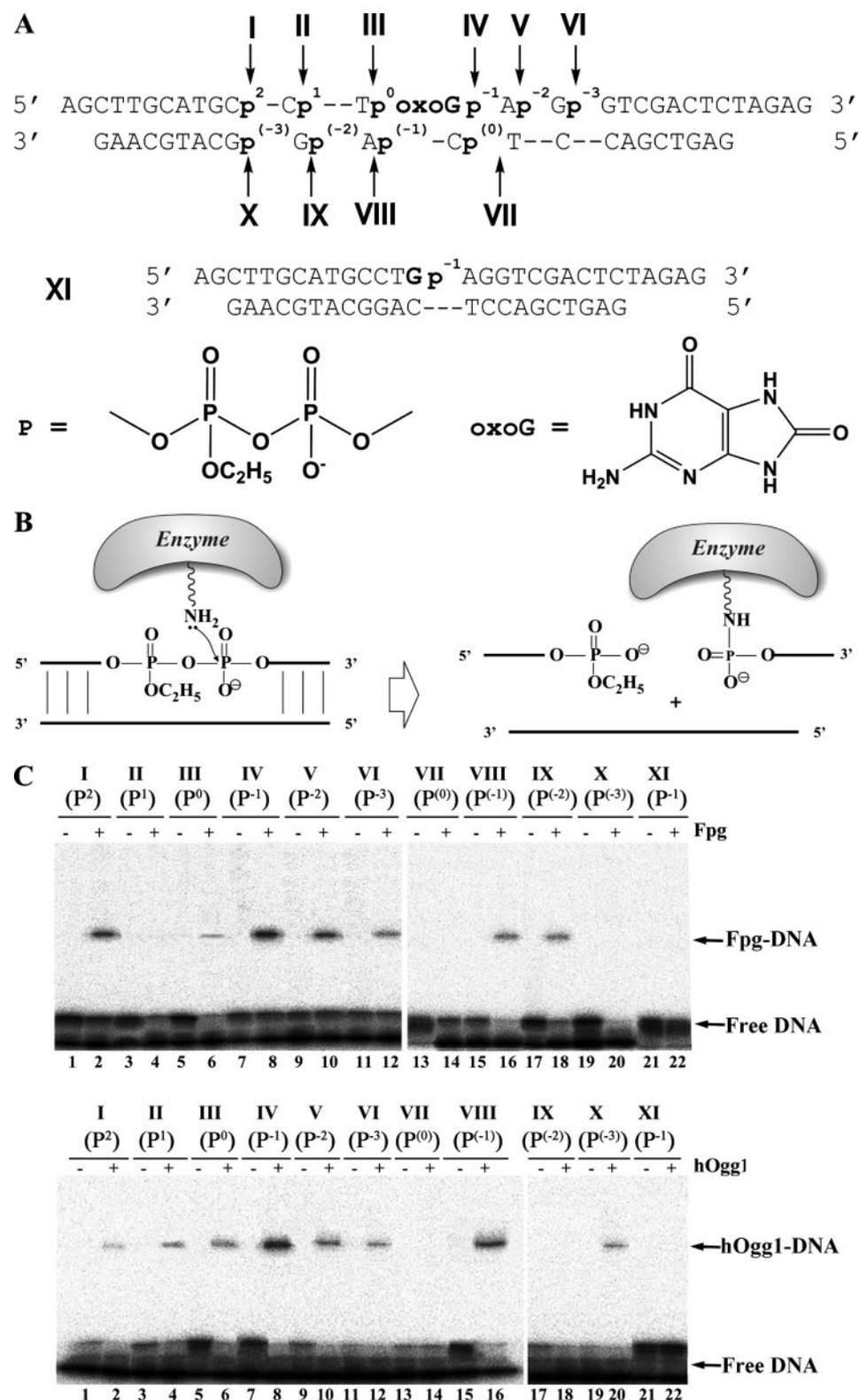
FIGURE 1. **Design and cross-linking properties of modified DNA duplexes.** *A*, scheme of phosphate-backbone modification of the double-stranded oligonucleotide containing an 8-oxoG residue and chemical structures of 8-oxoguanine and *O-ethyl*-pyrophosphate groups. The SPI positions are indicated by the boldface letter *p*; control duplex XI containing regular guanine is shown separately. *B*, scheme of the cross-linking reaction. *C*, cross-linking of modified DNA duplexes to *E. coli* Fpg (*top*) and human hOgg1 (*bottom*) proteins.

a histidine is cleaved by treatment with *N*-MeIm, whereas the bond between DNA phosphate and other nucleophilic amino acids is stable under these conditions (25). We also have established that DNA duplexes bearing SPI groups can cross-link with nucleophilic amino acids from DNA-binding enzymes situated within the DNA interface under near-physiological conditions (16, 23–26). More recently, it has been shown that Fpg can cover six nucleotides on the damaged strand and also make contacts with the complementary strand (27). We introduced single reactive SPI groups within an 8-oxoG-containing hexanucleotide sequence in the lesion-containing strand and at four positions of the opposite complementary strand.

Modeling of oligonucleotide duplex containing an SPI group using a combined quantum mechanical-molecular mechanical approach has revealed that stacking and Watson-Crick interactions between base pairs flanking the SPI group were not significantly affected.[3] Interestingly, the SPI group fits into the helix structure without elongation of the internucleotide distance, due to flipping out of the bi-substituted phosphate. The bi-substituted and tri-substituted phosphorus atoms of an SPI group are situated with respect to the native phosphorus atom of analogous nonmodified duplex DNA, at distances of about 2.3 and 1.3 Å, respectively.[3]

Chemical Cross-linking of DNA Duplexes Containing O-Ethyl-substituted Pyrophosphate Groups to the Fpg and hOgg1 Proteins—Oligonucleotide duplexes I–X structurally resemble the natural substrates of Fpg and hOgg1. Indeed, we have shown that both of these DNA glycosylases recognize and specifically bind to DNA duplexes with identical nucleotide sequences but bearing SPI groups at various positions (13, 16). To probe specific contacts between DNA phosphate groups and the proteins we used a chemical

stable in alkaline solution (0.1 M NaOH), but are hydrolyzed by treatment with acids (0.1 M HCl, 15% CH₃COOH) (24). Importantly, the covalent bond between a DNA phosphate group and

cross-linking approach. Reactions were carried out according to the scheme shown in Fig. 1*B*. The enzymes were incubated with internally labeled DNA duplexes I–X in the buffer used for

TABLE 1

Cross-linking efficiency of the DNA phosphate group to the *E. coli* Fpg and human hOgg1 proteins

Cross-linking efficiency values were determined as the ratio of the radioactivity of the cross-linking products to the total radioactivity. Optimal conditions are: 50 pM DNA duplex, 10 nM Fpg, 50 nM hOgg1, 14-h reaction time, temperatures are shown in the table. (−MeIm) and (+MeIm) indicate whether maximal cross-linking efficiency was achieved without or with the presence of *N*-MeIm, respectively. The cross-linking experiments were repeated three times and gave reproducible results (±10%). For structures see Fig. 1*A* and for more details see "Experimental Procedures."

	DNA duplex										
	I	II	III	IV	V	VI	VII	VIII	IX	X	XI
Protein	P^2	P^1	P^0	P^{-1}	P^{-2}	P^{-3}	$P^{(0)}$	$P^{(-1)}$	$P^{(-2)}$	$P^{(-3)}$	P^{-1}
Fpg	30% 22 °C +MeIm	0%	10% 22 °C +MeIm	50% 37 °C +MeIm	35% 37 °C +MeIm	18% 22 °C +MeIm	0%	20% 22 °C +MeIm	22% 22 °C +MeIm	0%	0%
hOgg1	6% 37 °C +MeIm	10% 37 °C −MeIm	15% 22 °C −MeIm	30% 37 °C +MeIm	15% 37 °C −MeIm	8% 37 °C −MeIm	0%	25% 37 °C −MeIm	0%	7% 37 °C +MeIm	0%

measuring DNA glycosylase activity. To optimize formation of the enzyme-substrate complex, we varied temperature, time of incubation, and concentration of reagents in the reaction mixture. It was shown previously that the addition of *N*-MeIm can lead to an increase in cross-linking efficiency (24). Therefore, the incubations were carried out in the presence or absence of *N*-MeIm. Optimal cross-linking conditions were found to be: 50 pM DNA duplex, 10 nM Fpg, 50 nM hOgg1, and 14-h reaction time. Maximum cross-linking efficiency of Fpg to all tested DNA duplexes, except IV and V, was achieved at 22 °C. Because DNA duplexes IV and V are non-cleavable substrate analogs, the maximum yield of protein cross-linking with these duplexes was obtained at 37 °C. In contrast with Fpg, maximum cross-linking efficiency of hOgg1 to all tested DNA duplexes, except III, was achieved at 37 °C. After covalent bond formation, the reaction mixtures were analyzed by 12% SDS-PAGE. As shown in Fig. 1*C* and Table 1, 7 and 8 phosphate groups in both strands of the oligonucleotide duplexes form covalent bonds with the Fpg and hOgg1 proteins, respectively. In both enzymes, the amino acids contact P^2, P^0, P^{-1}, P^{-2}, and P^{-3} phosphates in the 8-oxoG-containing strand and $P^{(-1)}$ phosphate in the complementary strand. In addition, hOgg1 covalently interacts with the P^1 and $P^{(-3)}$ phosphate groups, and Fpg with the $P^{(-2)}$ phosphate.

It is expected that cross-linking of the Fpg and hOgg1 proteins with DNA duplexes I–X occur in a specific manner because of the presence of the 8-oxoG residue (13, 18). Consistent with this observation, oligonucleotide duplex XI bearing an SPI group in the same position as duplex IV, but having no 8-oxoG residue, failed to cross-link with Fpg and hOgg1 (Fig. 1*C*).

Cross-linking efficiency ranged from 6 to 50% depending on the position of the SPI group in the duplex, incubation time, temperature, and *N*-MeIm presence or absence (Fig. 1*C*, Table 1 and data not shown). Such differences in the yields of cross-linked complexes might be due to the nature of the amino acids forming the covalent bond, their spatial orientation, and the availability in the amino acids of functional groups for the nucleophilic attack. Interestingly, the most efficient covalent complex formation, 50 and 30% for Fpg and hOgg1, respectively, was observed with duplex IV at 37 °C in the presence of 0.05 M *N*-MeIm. Together our data establish that, out of 10 phosphate groups shielded by the DNA glycosylases during base excision, 7 and 8 phosphate groups of the damaged strand

interact with nucleophilic amino acids of Fpg and hOgg1, respectively.

Identification of Lys^{249} as the hOgg1 Amino Acid Covalently Bound to DNA Duplex IV—We used a proteomics approach to identify the amino acid of hOgg1 that participates in cross-linking to the phosphate situated 3′ to 8-oxoG. We isolated cross-linked hOgg1 and free hOgg1 by separating these proteins by SDS-PAGE and cutting the respective bands from the gel. Cross-linked hOgg1 and free hOgg1 were alkylated with iodoacetamide and subsequently digested with trypsin in-gel. Peptides extracted from the gel slices were analyzed by ESI-MS/MS. According to the x-ray data on mutant catalytically inactive forms of hOgg1 in complex with 8-oxoG-containing DNA, amino acid residue Lys^{249} of hOgg1 would be the main candidate for interaction with P^{-1}. Trypsin digestion of free hOgg1 protein yielded two peptides flanking the Lys^{249} residue (^{239}ALCILPGVGT**K**^{249} and ^{250}VADCICLMALDKPQAVPVD-VHMWHIAQR^{277}; see Fig. 2, *A* and *B*, for the MS2 spectra confirming the identity of these peptides). Comparison of the presence of these peptides in free *versus* cross-linked proteins showed significant reduction in the amounts of these peptides in the cross-linked sample (the 239–249 peptide was almost absent and the amount of the 250–277 peptide was reduced 300-fold). In contrast, the amounts of peptide ^{214}AILEEQGGLAWLQQLR^{229}, which was not expected to cross-link to DNA, decreased only 30-fold in the sample with cross-linked protein (Fig. 2*C* for MS/MS confirmation of peptide identity), reflecting lesser amounts of hOgg1 protein in the cross-linked sample. Thus we observed at least a 10-fold decrease in the amounts of target peptides in the cross-linked sample compared with control peptide. Concerning the presence of negligible amounts of the target peptides in the cross-linked sample, one can account for their detection by spontaneous de-cross-linking of the oligopeptide conjugate induced by low pH during the sample preparation (24). Because for the peptide ^{239}ALCILPGVGT**K**^{249} the only nucleophilic residue is Lys^{249}, we conclude that this lysine cross-links to the phosphate located 3′ to the 8-oxoG residue.

Identification of the Peptide from Fpg That Is Coupled to DNA Duplex IV—To monitor formation of the covalent Fpg/oligonucleotide duplex IV complex, the reaction mixture was spiked with small amounts of ^{32}P-labeled DNA duplex IV. The Fpg-oligonucleotide cross-link reaction mixture was treated with chymotrypsin for 0, 3, and 14 h and the products of proteolytic digestion were analyzed by 12% denaturing PAGE and autora-
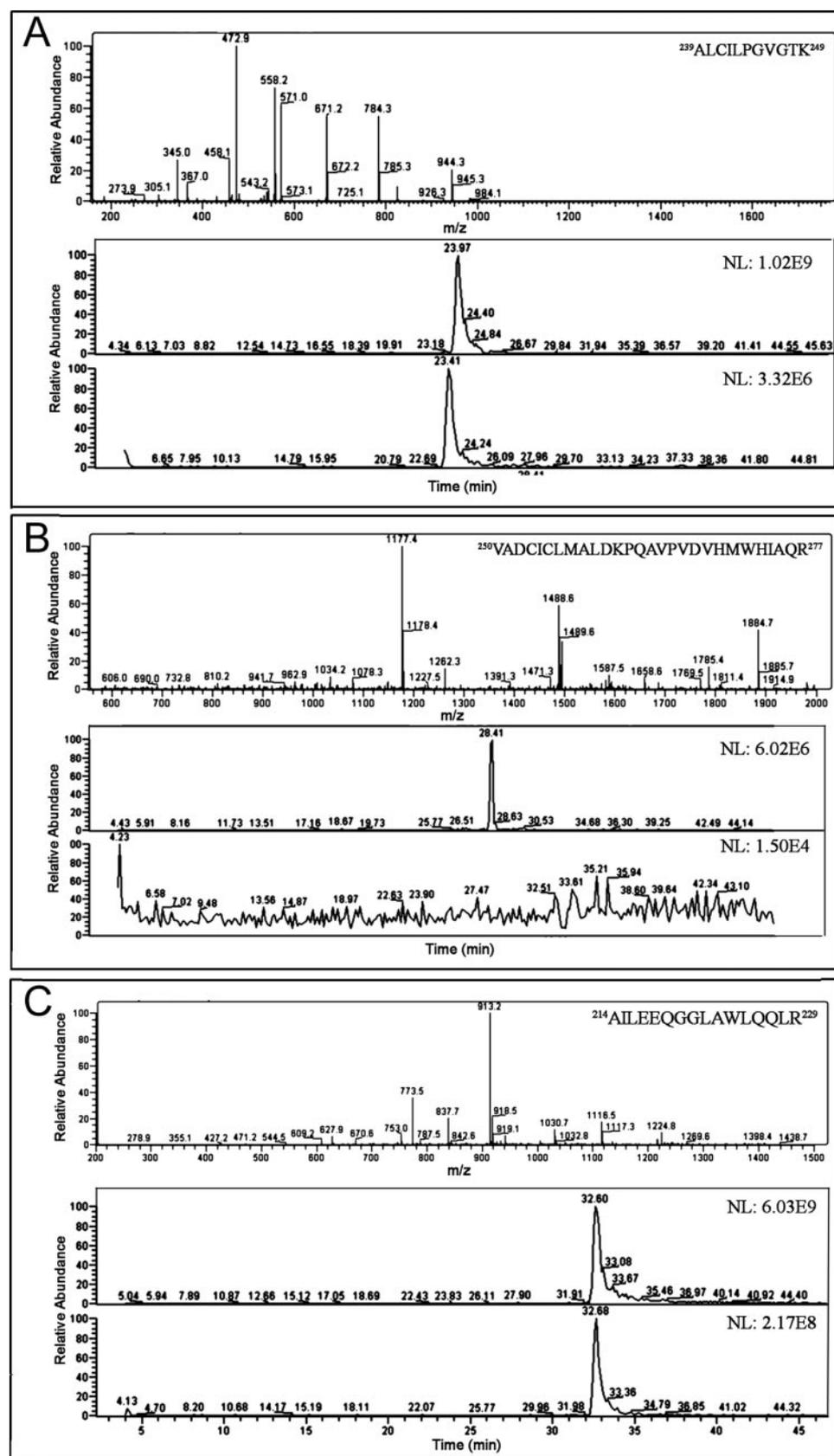
The Journal of Biological Chemistry

FIGURE 2. **Subtraction analysis of hOgg1-DNA interaction.** The *top* of each panel shows the MS/MS spectrum of the peptides derived from tryptic digestion of hOgg1. The sequences of peptides are indicated on the *top right corner*. The *middle* and *bottom* segments of each panel show the LC chromatograms of the corresponding peptides in the samples of free (*middle*) and cross-linked proteins (*bottom*). The peak intensity (total ion current), reflecting the peptide amount, is indicated on the *top right corner* of the segments.

diography. As shown in Fig. 3, about 50% of labeled oligonucleotide, corresponding to the cross-linked Fpg-DNA complex, migrates at the top of the gel (*lane 1*). Partial proteolysis of the covalent complex generates several chymotryptic peptide-oligonucleotide adducts, which migrate more slowly than the free DNA duplex (*lane 2*). Prolonged incubation with chymotrypsin converts all intermediate-sized Fpg-derived heteroconjugates to a single fast migrating peptide-DNA adduct (*lane 3*), suggesting that DNA duplex IV forms a cross-link with a single specific site in the Fpg protein.

To prepare the sample for mass spectrometry, the peptide-oligonucleotide heteroconjugate was separated from non-cross-linked peptides by anion exchange Q-Sepharose column chromatography, giving a 95% yield of DNA relative to input, and then de-cross-linked from DNA by treatment with 5% formic acid. Resulting samples were analyzed by nano-LC/MS, which revealed signals at *m/z* 504.3, 768.4, and 531.6 corresponding to the doubly charged protonated species of the [50]SVQRRA**KY**[57], [157]LMND-KLVVGVGNIY[170], and [207]RSIEQG-GTTL[217] peptides, respectively. MS/MS analysis confirmed the identity of these peptides (see Fig. 4 for the MS/MS spectrum of the [50]SVQRRA**KY**[57] peptide, and Fig. 6C for the [157]LMNDKLVVGVG-NIY[170] peptide). The [50]SVQR-RA**KY**[57] peptide contains Lys[56], which is expected to be involved in the interaction. Interestingly, although this was the suspected peptide, the two other peptides gave better and more intense signals than [50]SVQRRA**KY**[57].

According to the denaturing PAGE analysis, only one Fpg-derived peptide is responsible for cross-linking to DNA (Fig. 3, *lane 3*). Therefore, the detection of two additional peptides in the purified sample might be due to their more efficient ionization, which would lead to a disproportional representation of small background amounts

of these peptides present in the sample. In addition, [157]LMND-KLVVGVGNIY[170] and [207]RSIEQGGTTL[217] contain several hydrophobic amino acids that can facilitate nonspecific binding of these peptides to the resin during the chromatographic step. To examine these possibilities, we developed and applied a stable isotope approach. As shown in Fig. 5, the principal scheme consists of: 1) formation of a complex between DNA and non-labeled Fpg followed by cross-linking; 2) addition of un-cross-linked ^{15}N-labeled Fpg; 3) followed by protein denaturation and protease digestion of the resulting mixture; 4) isolation of the oligonucleotide-peptide heteroconjugate by chromatography; 5) hydrolysis of the covalent bond between the oligonucleotide and the peptide; and 6) identification of the resulting peptide by ESI-MS. The mass spectrometer was set to detect each candidate peptide and its heavy ^{15}N-containing variant. Both versions of the suspect peptides, [158]LMNDKLVVGVGNIY[171] and [208]RSIEQGGTTL[217], were easily detected in the sample (Fig. 6B and data not shown). The MS/MS analysis used to confirm their identity gave predicted shifts of mass (Fig. 6, C and D, and data not shown). Because the ^{15}N-labeled protein did not undergo cross-linking, we conclude that the presence of these two peptides in the purified sample does not require cross-linking to DNA. Therefore, they appear as a result of nonspecific binding and/or high ionization ability. On the other hand, we did not detect the ^{15}N-labeled variant for the expected peptide [50]SVQRRAKY[57] (Fig. 6A), indicating that the presence of the [50]SVQRRAKY[57] peptide in the analyzed sample is due to its cross-linking to DNA.

Mutational Analysis of Nucleophilic Amino Acids from [50]SVQRRAKY[57] That Can Cross-link to DNA Duplex IV—Because the covalent bond formation between protein and DNA duplex containing an SPI group requires nucleophilic amino acids, Lys[56], Arg[53], and Arg[54] residues present in the identified peptide are potential candidates. To find out which amino acid of the [50]SVQRRA**K**Y[57] peptide reacts with the phosphate 3′ to 8-oxoG, we tested the cross-linking abilities of Fpg mutants carrying amino acid substitutions R53G, R54G, K56R, or K56G, respectively. It was shown previously that these mutations do not affect the secondary structure of the protein; however, they do destabilize its tertiary structure somewhat (28, 29). The ability of mutant FpgK56R, FpgK56G, FpgK54G, and FpgK53G proteins to bind DNA duplex IV was investigated using an electrophoretic mobility shift assay (21, 22). Although DNA duplex IV cannot be cleaved by Fpg (18), binding assays and gel electrophoresis were performed at 0 and 4 °C, respectively. As shown in Fig. 7B, all mutant Fpg proteins tested form single specific complexes with DNA-duplex IV. The K_D values of mutant proteins for this DNA duplex were determined as described (21, 22). A representative experiment and results of quantitative analyses are shown in Fig. 7A and Table 2. Fig. 7A shows that incubation of DNA duplex IV with increasing concentrations of FpgK54G produces increased amounts of a band with reduced electrophoretic mobility, presumably a 1:1 FpgK54G-DNA duplex IV complex. Such experiments were used to determine the K_D values (21, 22). Table 2 shows that FpgK56G, FpgK54G, and FpgK53G mutants are significantly affected for DNA duplex IV binding compared with
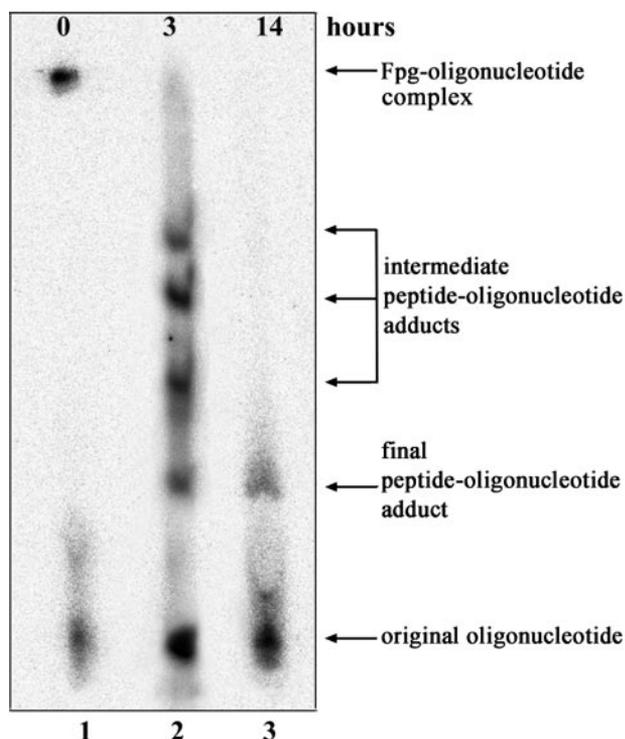

FIGURE 3. **Proteolytic digest of the Fpg-DNA complex.** Shown is the autoradiograph of the covalent Fpg-oligonucleotide complex, separated by 2 M urea gel electrophoresis. Aliquots of the Fpg-DNA conjugate were analyzed before (*lane 1*) and after 3 or 14 h of chymotrypsin digestion (*lanes 2 and 3*, respectively).
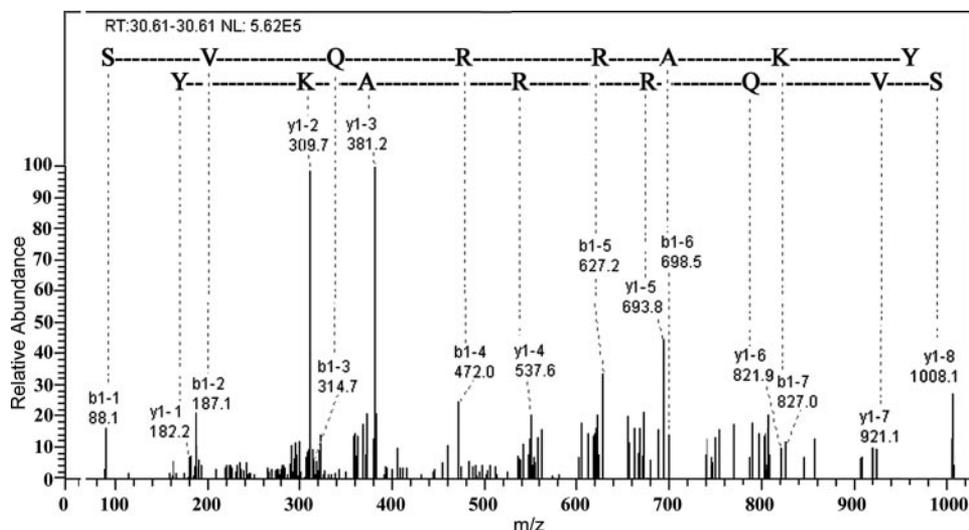

FIGURE 4. **MS/MS spectrum of the [50]SVQRRAKY[57] peptide.** The oligonucleotide-peptide conjugate was obtained by treatment of the crude reaction mixture of DNA-duplex IV and Fpg with chymotrypsin for 14 h and purification by anion-exchange chromatography, followed by desalting. After the de-cross-linking with 5% formic acid, the sample was analyzed on LC/MS/MS.
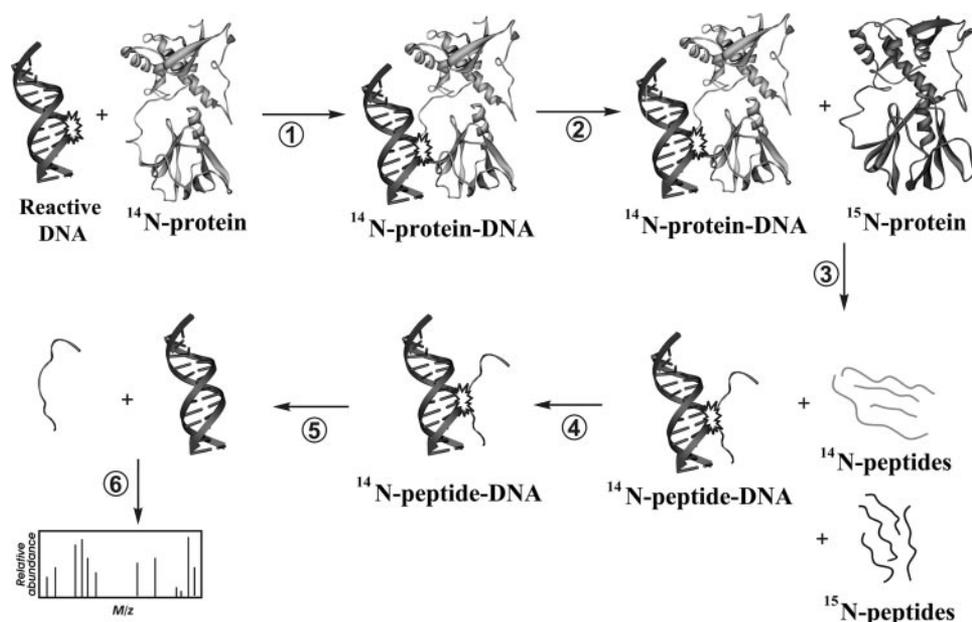
FIGURE 5. **Scheme of the stable isotope approach.** *1*) Formation of complex between DNA and non-labeled Fpg followed by cross-linking; *2*) addition of uncross-linked ^{15}N-labeled Fpg; *3*) denaturation and protease digestion of the resulting mixture; *4*) isolation of the oligonucleotide-peptide heteroconjugate by chromatography; *5*) hydrolysis of the covalent bond between the oligonucleotide and the peptide; *6*) identification of the resulting peptide by ESI-MS/MS. The mass spectrometer was set to detect each candidate peptide and its heavy ^{15}N-containing variant.

the wild-type Fpg. The K_D values of these three mutants are about 10-fold higher compared with that of wild-type Fpg. As expected from the similar properties of lysine and arginine residues, the FpgK56R mutant protein exhibited only a slight decrease in its binding affinity toward DNA duplex IV compared with the wild-type protein. As shown in Fig. 7C, the FpgK56R, FpgK53G, and FpgK54G mutants, in contrast to FpgK56G, cross-link to DNA duplex IV. This indicates that Lys^{56} in the ^{50}SVQRRA**K**Y^{57} peptide interacts with the DNA phosphate group 3′ to 8-oxoG. As shown in Table 2, the binding constants of the K56G, K54G, and K53G mutant Fpg proteins were comparable with each other. These results rule out the possibility that the inability of the K56G mutant to form a cross-link could be due to its poor binding to DNA compared with the other mutants.

Model of the Interaction between DNA Glycosylases and Internucleotide Phosphate Groups—Based on published structures and our cross-linking data, we propose the interaction scheme between DNA glycosylases and 8-oxoG-containing DNA duplex shown in Fig. 8. Our model of the protein-DNA contacts is based on the following rules: (i) hydrogen bonding can occur only at distances of no more than 3.2 Å between the respective atoms in DNA and proteins; (ii) van der Waals bonds can be formed only if the interacting atoms in both molecules are at a distance of no more than 4.5 Å. We also took into consideration the fact that the reactive phosphorous atom of the SPI group is displaced on 2.3 Å toward the C5′ atom compared with the phosphorous atom in native duplex DNA; however, the sugar-phosphate backbone of DNA at the site of modification has an increased flexibility due to the greater mobility of a pyrophosphate group compared with a natural phosphate.[3]

As seen in Fig. 8A, Fpg forms contacts with two phosphates (P^2 and P^0) at the 5′ end and with three consecutive phosphates (P^{-1}, P^{-2}, and P^{-3}) at the 3′ end of the damaged nucleotide. In addition, the four phosphates ($P^{(0)}$, $P^{(-1)}$, $P^{(-2)}$, and $P^{(-3)}$) in the complementary DNA strand are involved in the interaction (Fig. 8A). Seven of these nine contacts have been identified using the cross-linking approach. Our model also provides information about amino acid residues involved in the interaction. An ϵ-amino group of Lys^{254} in the zinc finger motif of Fpg interacts with the P^2 phosphate located two nucleotides 5′ to 8-oxoG. Three highly conserved amino acids (Arg^{258} in the zinc finger motif, Tyr^{236} in the flexible polypeptide hinge, which participates in the recognition of the damaged base, and Asn^{168} in the H2TH motif) specifically interact with the P^0 phosphate immediately upstream of 8-oxoG, with Arg^{258} being the most likely candidate for cross-linking, because the SPI groups in DNA are targeted only by nucleophilic amino acids. The highly conserved Lys^{56} residue interacts with the P^{-1} and P^{-2} phosphates, the distances from the ϵ-amino group of Lys^{56} to the P^{-1} and P^{-2} phosphates being 2.5 and 2.7 Å, respectively. The highly conserved residue His^{70} also interacts with P^{-2}; however, as attested by the positive effect of *N*-MeIm on cross-linking efficiency (16, 25), it appears not to be responsible for cross-linking. Arg^{33} contacts the P^{-3} phosphate two nucleotides downstream of 8-oxoG. Arg^{109}, which forms part of a reading head of Fpg to scan DNA for damage (35), contacts $P^{(-1)}$ phosphate in the complementary strand. The Lys^{88} residue is a candidate for making a covalent bond with the $P^{(-2)}$ atom, because its ϵ-amino group is located 3.1 Å from the $P^{(-2)}$ atom.

Fig. 8B presents the model for hOgg1 interaction with the 8-oxoG-containing DNA duplex. This protein makes contacts with three phosphates (P^2, P^1, and P^0) that are 5′ to 8-oxoG, three phosphates (P^{-1}, P^{-2}, and P^{-3}) that are 3′ to 8-oxoG (Fig. 8B), and two consecutive phosphates ($P^{(-1)}$ and $P^{(-3)}$) in the complementary DNA strand (Fig. 8). We propose that nucleophilic amino acids in the amino- and carboxyl-terminal fragments of hOgg1 participate in contacts with the opposite DNA strand. Indeed, these fragments have been deleted to obtain co-crystals of hOgg1K249Q and 8-oxoG·C-DNA (8). Consistent with our findings, the core domain of hOgg1 exhibits lower DNA binding affinity compared with the full-length protein (8, 34). Interestingly, the modified P^0, P^{-2}, and P^{-3} phosphates exhibit maximal cross-linking efficiency to hOgg1 in the absence of *N*-MeIm, suggesting that histidine residues are involved in covalent
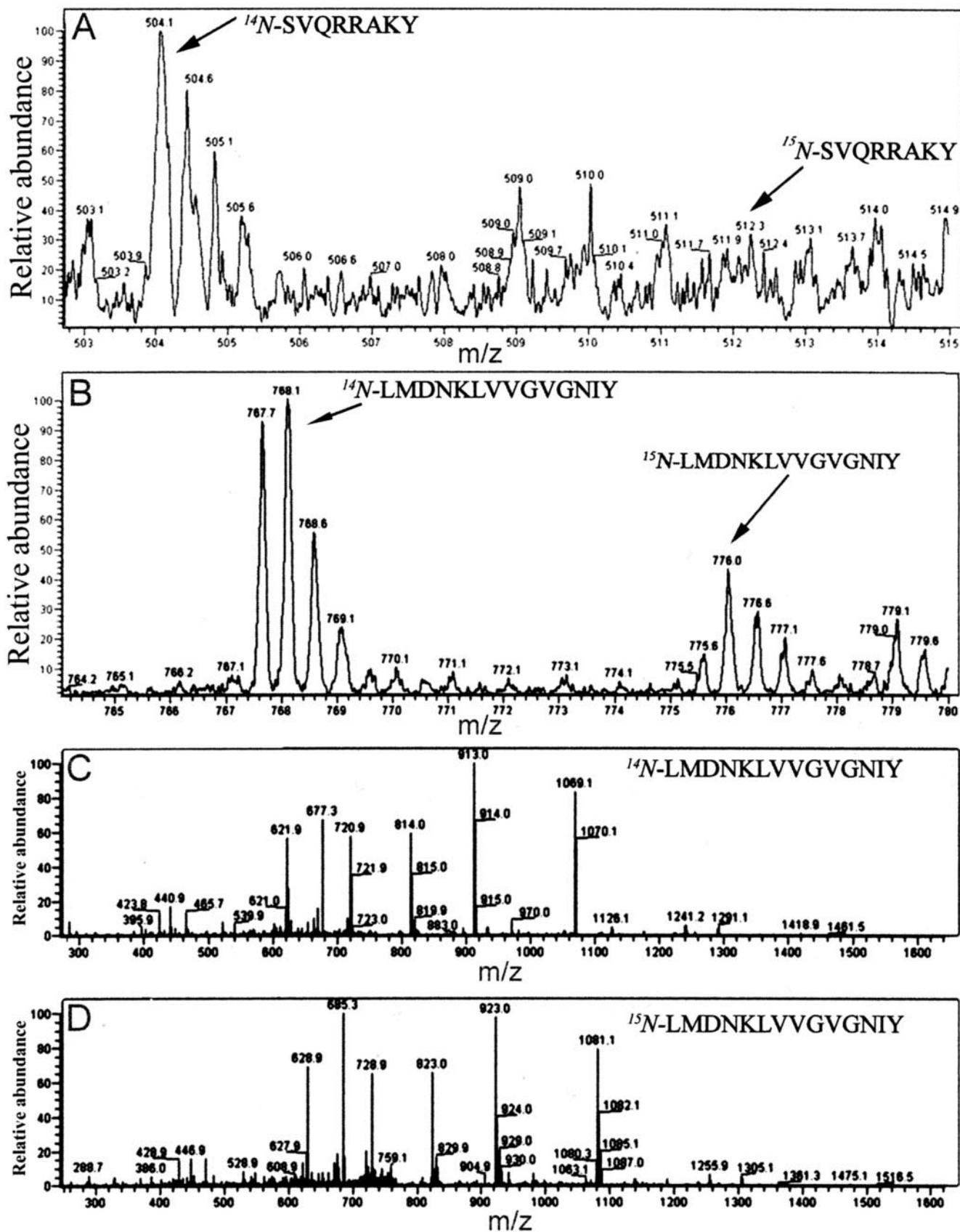
FIGURE 6. **Enrichment analysis of Fpg-DNA interaction using stable isotope labeling.** *A* and *B*, shown are the zoom scans of the peaks corresponding to the [50]SVQRRAKY[57] and [157]LMDNKLVVGVGNIY[17] peptides after their LC/MS/MS analysis. The ions corresponding to both light and heavy versions of the peaks (including the expected position of the heavy [50]SVQRRAKY[57] peak) are indicated by *arrows*. *C* and *D*, MS/MS spectra of the light and heavy versions of the [157]LMDNKLVVGVGNIY[17] peptide, confirming their identity.
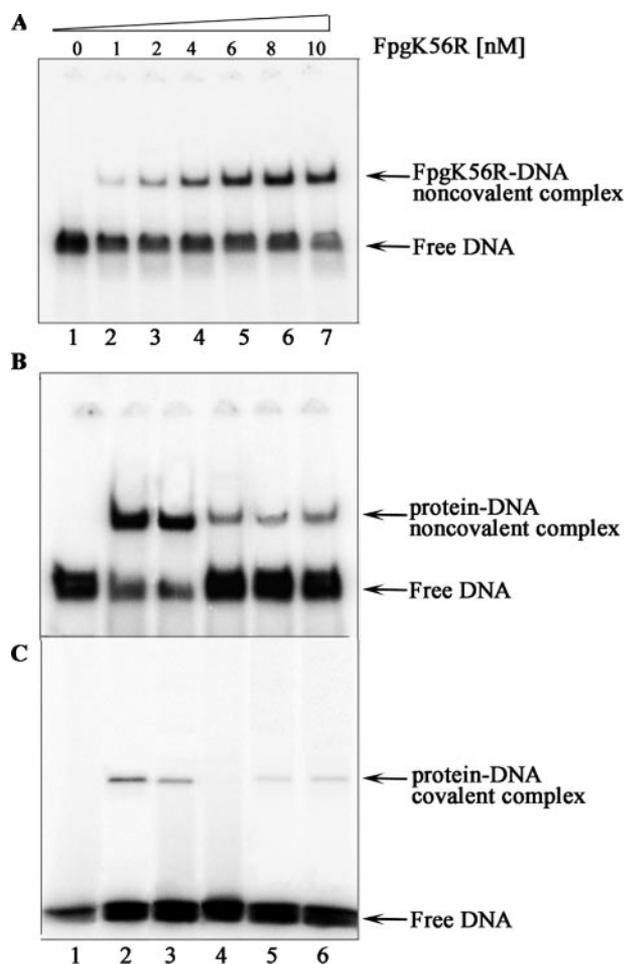
FIGURE 7. **Mutational analysis of Fpg-DNA binding.** *A*, binding of FpgK56R to DNA duplex IV. Electrophoretic mobility shift assay was performed using 20 pM DNA duplex IV and 1, 2, 4, 6, 8, and 10 nM FpgK56R (*lane 2–7*, respectively). Non-covalent (*B*) and covalent (*C*) binding of DNA-duplex IV to wild-type Fpg, and mutants FpgK56R, FpgK56G, FpgK53G, and FpgK54G (*lanes 2* and *3–6*, respectively). *Lane 1* on each gel corresponds to control DNA-duplex IV.

TABLE 2

Binding constant for DNA-duplex IV with wild-type Fpg and mutant K56R, K56G, R53G, and R54G

Protein	Fpg	K56R	K56G	R53G	R54G
K_D, nM[a]	3.0 ± 0.6	7.0 ± 0.6	48.0 ± 5.0	35.0 ± 2.0	20.0 ± 0.9

[a] K_D values were determined by electrophoretic mobility shift assay as described under "Experimental Procedures." DNA concentration was 20 pM and the protein concentration ranges were 0.1–12, 1–10, and 1–100 nM for wild-type Fpg, FpgK56R and FpgK56G, FpgR53G, FpgR54G, respectively. The mean ± S.D. of three independent experiments are shown.

bond formation. We suggest that P^0 contacts His^{270} in the HhH-GPD motif. Conserved and functionally significant Lys^{249} could interact with the P^{-1} atom, due both to the distance (4.4 Å) between its ϵ-amino group and the phosphate group and to the positive effect of *N*-MeIm on cross-linking. Whereas the co-crystal structure reveals that the P^{-2} atom contacts the main chain of Val^{250} and Lys^{249}, and the highly conserved Gly^{245} residue in the HhH motif forms a hydrogen bond with P^{-3}, our cross-linking data clearly demonstrate that the P^{-2} and P^{-3} phosphates interact with nucleophilic amino acids, most likely with histidine residues, in hOgg1.

DISCUSSION

Endogenous oxidative DNA lesions are most abundant and inevitable as cells generate reactive oxygen species through aerobic respiration. A common base modification formed by oxidation of guanine at C-8 is 8-oxoG, a major mutagenic DNA lesion, which results either from direct oxidation of guanines in DNA or misincorporation of 8-oxo-dGTP by DNA polymerases causing mainly G·C to T·A transversions. *E. coli* Fpg and its functional homologue Ogg1 in human cells initiate the base excision repair pathway to remove this lesion from duplex DNA. Despite progress in crystallographic studies of Fpg and hOgg1, several critical questions remain unanswered. How does a DNA glycosylase locate the lesion amid the enormous excess of native bases, and what are the mechanisms by which the enzyme discriminates between appropriate and inappropriate substrate bases? Importantly, the crystallographic data can differ from those obtained in biochemical experiments because the latter are carried out in solution under near-physiological conditions. Here we combined cross-linking and MS approaches to study the cross-linked complexes of Fpg and hOgg1 on DNA duplexes containing a single 8-oxoG residue and a reactive SPI group.

Formation of covalent complexes of Fpg and hOgg1 with DNA substrate analogs provides direct evidence for docking between nucleophilic groups of amino acids and internucleotide phosphates. We examined two covalent Fpg-DNA and hOgg1-DNA complexes resulting from cross-linking of the proteins to DNA duplex IV bearing a modified internucleotide P^{-1} group downstream to 8-oxoG. DNA duplex IV could be of interest as a specific inhibitor of 8-oxoG-DNA glycosylases, because we have shown previously that this synthetic molecule is a non-cleavable substrate analog for Fpg and hOgg1, which bind specifically to the duplex but do not cleave it (16). These types of inhibitors might prove useful in cancer chemotherapy (36, 37). In addition, such modified DNA duplexes could be used in structural and mechanistic studies of DNA damage recognition. The high cross-linking yields using this duplex greatly facilitate the MS analysis.

This paper presents two approaches to combining cross-linking and ESI/MS/MS to study covalent protein-DNA complexes. The first approach can be called the "subtraction" approach. It is based on comparison of the mass spectra of peptides originating from cross-linked and non-cross-linked proteins. We expected that the peptide spectrum for the cross-linked protein would not contain any peptide bearing an amino acid involved in formation of the covalent bond with DNA, because of changes in its mass and ionization properties upon cross-linking. At the same time, the mass spectrum of the control non-cross-linked protein should contain all detectable peptides. Using this approach, we have demonstrated that two peptides flanking the candidate Lys^{249} of the hOgg1 protein become markedly underrepresented after cross-linking, thus confirming the identity of the amino acid residue predicted from our model of hOgg1 binding.

However, use of the subtraction approach to study the Fpg-DNA complex was significantly more difficult than for the hOgg1-DNA complex. In our experiments, trypsin-generated
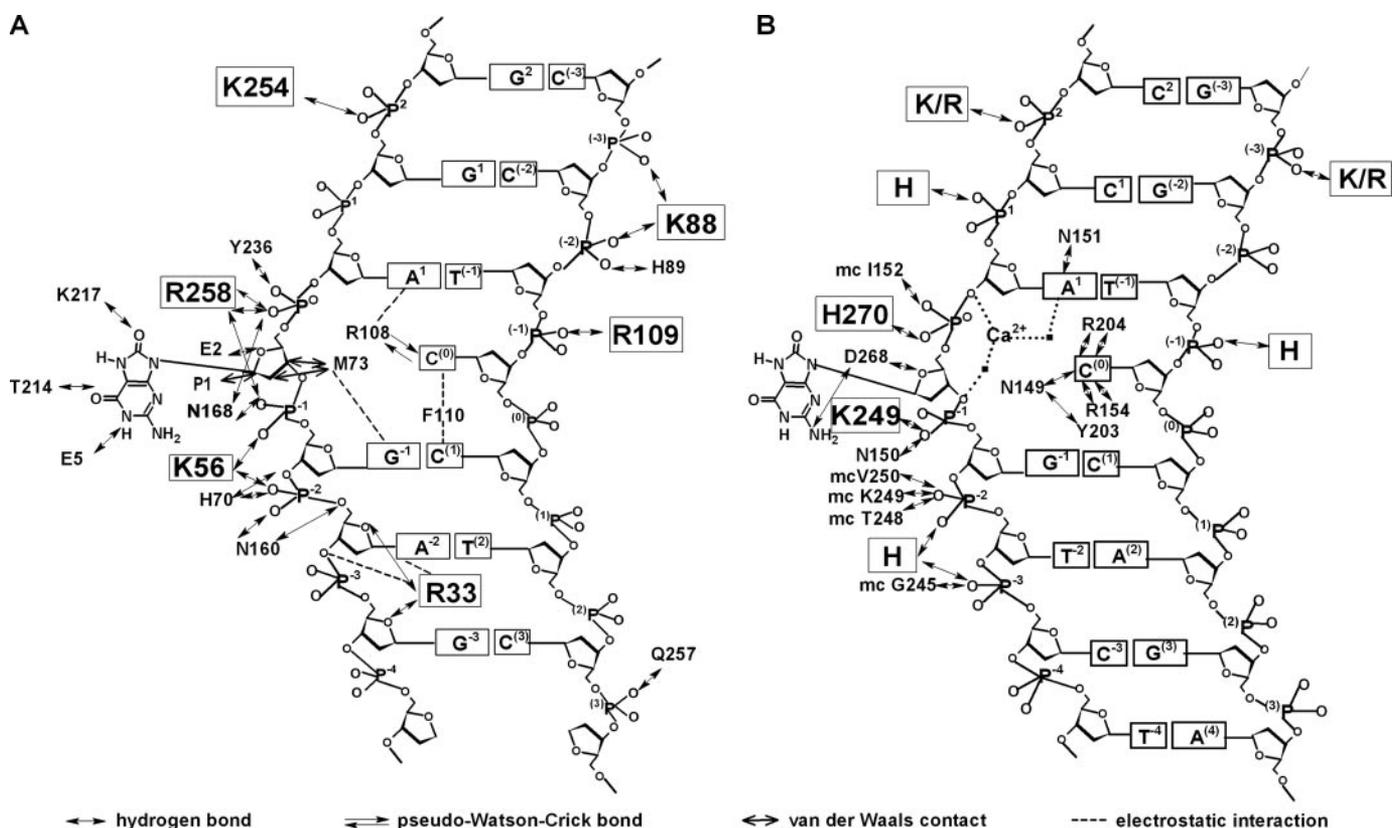
A **B**

← → hydrogen bond   ⇒ pseudo-Watson-Crick bond   ↔ van der Waals contact   ---- electrostatic interaction

FIGURE 8. **Model of Fpg-DNA and hOgg1-DNA interaction.** Schematic representation of contacts of DNA phosphates groups with Fpg protein (*A*) and hOgg1 (*B*) based on experimental data from this article and from the literature. The central nucleotides of the lesion-containing and complementary strands are 8-oxoG[0] and -C[(0)], respectively. Nucleotides are numbered as shown with those in the complementary strand in *parentheses*. Arginine 108 forms pseudo-Watson-Crick interactions (hydrogen bonds) between its Nη-1 and Nϵ atoms and the N-3 and O-2 of the estranged cytosine (C[(0)]), respectively. Also see Ref. 31.

peptides [55]AK[56] and [57]YLLLELPEGWIIIHLGMSGSLR[78], and chymotrypsin-generated peptide [50]SVQRRAKY[57] all containing the candidate Lys[56] residue were not detected in the digest of control free protein (data not shown). Most likely, this was due to the poor ionization properties of these peptides, exacerbated by ionization suppression caused by the presence of other peptides in the mixture. Therefore, we tried a complementary "enrichment" approach. Specifically, we purified oligonucleotide-peptide heteroconjugate, reversed the peptide-DNA cross-link, and analyzed the resulting peptides by MS. The advantage of reactive SPI groups is that they form covalent bonds that are readily and selectively decomposed, yielding peptides ready for MS analysis. In our protocol, we cleaved the covalent phosphoamide bond between peptides and oligonucleotides by treatment with 5% formic acid. Strikingly, we were able to detect the [50]SVQRRAKY[57] peptide in the mass spectrum of a proteolytic digest of the Fpg-DNA complex, suggesting that this peptide was enriched after cross-linking followed by heteroconjugate purification and became visible in the absence of competitor peptides.

In addition to the expected [50]SVQRRAKY[57] peptide, however, two other peptides ([158]LMNDKLVVGVGNIY[171] and [208]RSIEQGGTTL[217]) were also detected in the purified sample. The [158]LMNDKLVVGVGNIY[171] peptide belongs to the DNA-binding H2TH motif. Amino acids in the [207]RSIEQGGTTL[217] peptide are part of the loop involved in recognition of the 8-oxoG residue. Intriguingly, these two peptides were found to

give better and more intense signals than the former one, raising the possibility that they could also cross-link to DNA. Alternatively, they might be detected because of nonspecific binding to the Q-Sepharose column and their superior ionization properties.

The dramatic variability in the ionization efficiency of chemically different molecules usually precludes quantitative comparison of the relative amounts of different peptides in a mixture. A general approach to address this problem is the use of stable isotope labeling, which takes advantage of the fact that ionization efficiency is determined by electron structure and generally is not affected by the nuclear mass. Various stable isotope labeling schemes have been developed for use in quantitative proteomics, such as ICAT and SILAC (38, 39). We used stable isotope labeling to control for nonspecific binding of the observed peptides. Metabolic labeling with ^{15}N was utilized to distinguish by mass the identical Fpg-derived peptides from control and experimental samples. ^{15}N-Labeled free Fpg protein was added to the mixture immediately after cross-linking unlabeled Fpg with the oligonucleotide, *i.e.* before the heteroconjugate purification step. All subsequent steps were performed with this mixture, ensuring that any differences in the amounts of ^{15}N- and ^{14}N-peptides that were detected by mass spectrometry could be attributed to the chemical cross-linking. Because ^{15}N-labeled Fpg did not undergo cross-linking, detection of ^{15}N-peptides in the purified sample served as an internal control for nonspecific binding and ionization efficiency.

Proteomics of DNA Glycosylase Interaction with Damaged DNA

Whereas we could easily detect the heavy variants of the [158]LMNDKLVVGVGNIY[171] and [208]RSIEQGGTTL[217] peptides in these experiments, we failed to detect the ^{15}N-labeled variant of [50]SVQRRA**K**Y[57], indicating that this peptide was cross-linked to DNA.

The [50]SVQRRA**K**Y[57] peptide contains three nucleophilic amino acids that could interact with the SPI group in duplex IV: Arg[53], Arg[54], and Lys[56]. Here, we used amino acid substitutions R53G, R54G, K56R, and K56G in Fpg mutants to identify the amino acid that reacts with the P^{-1} atom. We investigated the efficacy of complex formation between the mutant Fpg proteins and duplex DNA carrying an SPI group 3′ to the 8-oxoG residue, and compared it with wild-type Fpg. Mutant FpgK56G, FpgR53G, and FpgR54G proteins exhibit a ~10-fold higher K_D than the wild-type protein. This suggests that Lys[56], Arg[54], and Arg[53] could be specifically implicated in the recognition and binding of the 8-oxoG-containing DNA. It is known that Arg[54] and Arg[53] form hydrogen bonds stabilizing the $\beta2$–$\beta3$ loop of Fpg and bringing together the amino- and carboxyl-terminal domains; loss of these interactions would affect positioning of Lys[56] (7). Among the Fpg mutants tested, only FpgK56G failed to cross-link with DNA duplex IV, indicating that Lys[56] is indeed the residue that interacts with the DNA phosphate group 3′ to 8-oxoG. Previously, we have studied the role of the conserved Lys[56] residue in the various catalytic activities of Fpg by site-specific mutagenesis (17, 40). The DNA glycosylase activity of FpgK56G toward 2,6-diamino-4-hydroxy-5-N-methylformamidopyrimidine residues is comparable with that of the wild-type enzyme (17). However, the FpgK56G mutant protein has dramatically reduced (55-fold) 8-oxoG-DNA glycosylase activity. Nevertheless, overexpression of the mutant protein partially restored the ability to prevent spontaneously induced G·C → T·A transversions in the repair-deficient *E. coli fpg mutY* strain. Unexpectedly, Lys[56] but not Pro[1] was crucial for excision of oxidatively damaged pyrimidines such as 5,6-dihydrothymine and fragmented thymine (40). These observations, together with our data, suggest that interaction of Lys[56] with the P^{-1} atom downstream of the modified base is essential for the catalytic steps of base excision.

At present, the crystal structures of wild-type Fpg and hOgg1 complexed with the 8-oxoG-containing DNA are not available. However, several co-crystal structures of hOgg1 and Fpg from different species with the AP site-containing DNA have been solved (7, 30–32). Moreover, three-dimensional structures of complexes between 8-oxoG-containing DNA and the mutant recognition-competent but catalytically inactive E3Q form of Fpg from *Bacillus stearothermophilus* (33) as well as truncated hOgg1 K249Q and D268N mutants have been obtained (8, 34). Based on the published structures together with our cross-linking data, we propose an interaction model between DNA glycosylases and 8-oxoG-containing duplex DNA. Because our models are consistent with the cross-linking results, we used DNA duplexes I–X to elucidate the amino acids of the protein interacting with internucleotide phosphates in damaged DNA.

The combined cross-linking and mass spectrometry approaches developed in this work proved to be fruitful in detecting specific contacts between DNA phosphate groups and 8-oxoG-DNA glycosylases of both bacterial and human origin.

The observations reported here confirm the results of crystallographic studies of hOgg1-DNA and Fpg-DNA complexes indicating that Lys[249] and Lys[56] in these DNA glycosylases interact with the phosphate group of DNA immediately downstream to the 8-oxoG residue. The present study provides evidence that, in solution under physiologically relevant conditions, the conformation of enzyme-substrate complexes much resembles that observed in the crystals. In addition, we have identified new specific contacts between nucleophilic amino acids in the active centers of Fpg and hOgg1 and internucleotide phosphates in damaged DNA, which were not seen in the co-crystals. Our data suggest that multiple interactions with DNA phosphate groups direct formation of specific Fpg-DNA and hOgg1-DNA complexes and play a critical role in substrate recognition. In conclusion, the improved methods developed in this work can be used to study complex DNA-protein interactions and help to further elucidate molecular mechanisms of DNA repair.

REFERENCES

1. Laval, J., Jurado, J., Saparbaev, M., and Sidorkina, O. (1998) *Mutat. Res.* **402,** 93–102
2. Tchou, J., Kasai, H., Shibutani, S., Chung, M. H., Laval, J., Grollman, A. P., and Nishimura, S. (1991) *Proc. Natl. Acad. Sci. U. S. A.* **88,** 4690–4694
3. Tchou, J., Bodepudi, V., Shibutani, S., Antoshechkin, I., Miller, J., Grollman, A. P., and Johnson, F. (1994) *J. Biol. Chem.* **269,** 15318–15324
4. Lindahl, T. (1993) *Nature* **362,** 709–715
5. Shibutani, S., Takeshita, M., and Grollman, A. P. (1991) *Nature* **349,** 431–434
6. Moriya, M., Ou, C., Bodepudi, V., Johnson, F., Takeshita, M., and Grollman, A. P. (1991) *Mutat. Res.* **254,** 281–288
7. Gilboa, R., Zharkov, D. O., Golan, G., Fernandes, A. S., Gerchman, S. E., Matz, E., Kycia, J. H., Grollman, A. P., and Shoham, G. (2002) *J. Biol. Chem.* **277,** 19811–19816
8. Bruner, S. D., Norman, D. P., and Verdine, G. L. (2000) *Nature* **403,** 859–866
9. Zharkov, D. O., Ishchenko, A. A., Douglas, K. T., and Nevinsky, G. A. (2003) *Mutat. Res.* **531,** 141–156
10. Kirpota, O. O., Zharkov, D. O., Buneva, V. N., and Nevinsky, G. A. (2006) *Mol. Biol.* (*Mosc.*) **5,** 512–523
11. Wong, S. S. (1991) *Chemistry of Protein Conjugation and Cross-linking*, 1st Ed., CRC Press, Boca Raton, FL
12. Back, J. W., de Jong, L., Muijsers, A. O., and de Koster, C. G. (2003) *J. Mol. Biol.* **331,** 303–313
13. Kuznetsova, S., Rykhlevskaya, A., Taranenko, M., Sidorkina, O., Oretskaya, T., and Laval, J. (2003) *Biochimie* (*Paris*) **85,** 511–519
14. Kuznetsova, S. A., Clusel, C., Ugarte, E., Elias, I., Vasseur, M., Blumenfeld, M., and Shabarova, Z. A. (1996) *Nucleic Acids Res.* **24,** 4783–4790
15. Gros, L., Ishchenko, A. A., Ide, H., Elder, R. H., and Saparbaev, M. K. (2004) *Nucleic Acids Res.* **32,** 73–81
16. Shabarova, Z. A., Sheflyan, G. Y., Kuznetsova, S. A., Kubareva, E. A., Sysoev, O. H., Ivanovskaya, M. G., and Gromova, E. S. (1994) *Bioorg. Khim.* **20,** 413–419
17. Boiteux, S., O'Connor, T. R., Lederer, F., Gouyette, A., and Laval, J. (1990) *J. Biol. Chem.* **265,** 3916–3922
18. Rogacheva, M. V., Saparbaev, M. K., Afanasov, I. M., and Kuznetsova, S. A. (2005) *Biochimie* (*Paris*) **87,** 1079–1088
19. Sidorkina, O. M., and Laval, J. (1998) *Nucleic Acids Res.* **26,** 5351–5357

20. Sidorkina, O. M., and Laval, J. (2000) *J. Biol. Chem.* **275,** 9924–9929
21. Castaing, B., Boiteux, S., and Zelwer, C. (1992) *Nucleic Acids Res.* **20,** 389–394
22. Castaing, B., Geiger, A., Seliger, H., Nehls, P., Laval, J., Zelwer, C., and Boiteux, S. (1993) *Nucleic Acids Res.* **21,** 2899–2905
23. Naryshkin, N. A., Farrow, M. A., Ivanovskaya, M. G., Oretskaya, T. S., Shabarova, Z. A., and Gait, M. J. (1997) *Biochemistry* **36,** 3496–3505
24. Purmal, A. A., Shabarova, Z. A., and Gumport, R. I. (1992) *Nucleic Acids Res.* **20,** 3713–3719
25. Rudakova, E. A., Ivanovskaya, M. G., Kozlov, M. V., Khoretonenko, M. V., Oretskaya, T. S., and Nikiforov, V. G. (2000) *Biochemistry* (*Mosc.*) **65,** 640–650
26. Sheflyan, G., Kubareva, E. A., Kuznetsova, S. A., Karyagina, A. S., Nikolskaya, I. I., Gromova, E. S., and Shabarova, Z. A. (1996) *FEBS Lett.* **390,** 307–310
27. Castaing, B., Fourrey, J. L., Hervouet, N., Thomas, M., Boiteux, S., and Zelwer, C. (1999) *Nucleic Acids Res.* **27,** 608–615
28. Kuznetsov, S. V., Sidorkina, O. M., Jurado, J., Bazin, M., Tauc, P., Brochon, J. C., Laval, J., and Santus, R. (1998) *Eur. J. Biochem.* **253,** 413–420
29. Sidorkina, O., Dizdaroglu, M., and Laval, J. (2001) *Free Radic. Biol. Med.* **31,** 816–823
30. Fromme, J. C., and Verdine, G. L. (2002) *Nat. Struct. Biol.* **9,** 544–552
31. Serre, L., Pereira de Jesus, K., Boiteux, S., Zelwer, C., and Castaing, B. (2002) *EMBO J.* **21,** 2854–2865
32. Norman, D. P. G., Bruner, S. D., and Verdine, G. L. (2001) *J. Am. Chem. Soc.* **123,** 359–360
33. Fromme, J. C., and Verdine, G. L. (2003) *J. Biol. Chem.* **278,** 51543–51548
34. Norman, D. P., Chung, S. J., and Verdine, G. L. (2003) *Biochemistry* **42,** 1564–1572
35. Zaika, E. I., Perlow, R. A., Matz, E., Broyde, S., Gilboa, R., Grollman, A. P., and Zharkov, D. O. (2004) *J. Biol. Chem.* **279,** 4849–4861
36. Speina, E., Ciesla, J. M., Graziewicz, M. A., Laval, J., Kazimierczuk, Z., and Tudek, B. (2005) *Acta Biochim. Pol.* **52,** 167–178
37. Wiederholt, C. J., Delaney, M. O., and Greenberg, M. M. (2002) *Biochemistry* **41,** 15838–15844
38. Gygi, S. P., Rist, B., Gerber, S. A., Turecek, F., Gelb, M. H., and Aebersold, R. (1999) *Nat. Biotechnol.* **17,** 994–999
39. Ong, S. E., and Mann, M. (2005) *Nat. Chem. Biol.* **1,** 252–262
40. Saparbaev, M., Sidorkina, O. M., Jurado, J., Privezentzev, C. V., Greenberg, M. M., and Laval, J. (2002) *Environ. Mol. Mutagen.* **39,** 10–17